Experimental test of kinetic theories for heterogeneous freezing in silicon

P. A. Stolk, A. Polman, and W. C. Sinke*
FOM-Institute for Atomic and Molecular Physics, Kruislaan 407, 1098 SJ Amsterdam, The Netherlands
(Received 26 August 1991)

The crystallization rate of liquid silicon has been measured during epitaxial explosive crystallization of amorphous silicon. The measurements, together with numerical temperature calculations indicate that freezing in silicon saturates at 15.8 m/s for large undercooling (> 130 K) below the equilibrium melting temperature. These data, as well as a variety of experimental results of other investigators, are used to test two models describing the kinetics of heterogeneous freezing. A transition-state theory in which the phase transformations are assumed to go through an intermediate state at a rate limited by the sound velocity is not consistent with the data. A theory in which the rate-limiting factor in freezing of liquid silicon is atomic diffusion in the liquid close to the interface describes the data well. The activation energy for self-diffusion of atoms in the liquid near the interface is found to be 0.7–1.1 eV.

I. INTRODUCTION

The nonequilibrium phase transformations that occur upon laser melting of semiconductors generally are heterogeneous, that is, they are governed by the motion of a solid-liquid interface that is undercooled (freezing) or overheated (melting) with respect to the equilibrium melting temperature (T_m).[1] The interface response function $v(T)$ describes the velocity at which the interface moves in response to overheating or undercooling. Determination of the response function could give insight into the atomic processes that lead to the phase transformations.

In the past decade, the interface response function of crystalline silicon (c-Si) has been investigated by time-resolved conductance measurements,[2–5] time-resolved x-ray scattering,[6] and picosecond-laser measurements.[3,7] Additionally, the c-Si/liquid Si (l-Si) system has been studied by molecular-dynamics simulations.[8–12] Despite these extensive studies, an unambiguous picture of the theory underlying melting and freezing in silicon has not been obtained so far.

In a macroscopic picture the interface velocity is determined by the difference in the rate at which atoms attach to (freezing) or detach from (melting) the solid at the interface. Two fundamentally different theories can be applied to describe the effective interface velocity as a function of the temperature. In the transition state theory (TST) it is assumed that transitions between the solid and liquid phase occur via an intermediate state, which introduces a transformation barrier in $v(T)$. In the diffusion limited theory (DLT) it is instead assumed that the interface velocity is related to the diffusivity of atoms in the liquid. For both theories the response function $v(T)$ can be represented by the following general expression:[1]

$$v(T)=c\exp(-Q/kT)[1-\exp(-\Delta g_{ls}/kT)]\ , \qquad (1)$$

where Δg_{ls} is the difference in Gibbs free energy per atom between the liquid and the solid, k is Boltzmann's constant, T the absolute temperature, and Q an activation energy. The kinetic prefactor c is given by $c=f\omega_0 d$, where ω_0 is an attempt frequency, d an average distance over which the interface moves for a successful jump, and f the fraction of active sites at the interface ($f\leq 1$). By convention, $v(T)$ is positive for freezing and negative for melting.

In the conventional "collision limited" growth model of TST the maximum freezing velocity is taken to be fundamentally limited by the sound velocity c_s in the solid:[4] $c\leq c_s$. In the "entropy limited" formulation of TST, the entropy difference Δs_{ls} between the liquid and solid introduces an additional barrier to freezing: $c\leq c_s\exp(-\Delta s_{ls}/k)$. This entropy barrier is related to the small volume in configurational and vibrational phase space for which transformation from the liquid to the solid phase is possible.[4] In this paper we will study solid-liquid transformations for crystalline and amorphous Si (a-Si). For c-Si $c_s=8433$ m/s is applicable, the measured longitudinal velocity of sound along the [100] direction. For a-Si no accurate experimental data exist,[13] hence we estimate, using published elastic properties of ion-implanted a-Si, $c_s\approx 8400$ m/s.[14]

In the DLT the collision frequencies at the interface are assumed to be limited by the diffusivity of atoms in the liquid.[15,16] Here the general form for $v(T)$, as given by Eq. (1), still holds but the parameters have a different physical meaning: Q represents the activation energy for self-diffusion of atoms in the liquid near the interface, and the attempt frequency ω_0 is given by D_0/λ^2, where λ is a characteristic diffusion distance and D_0 the prefactor in the equation for the diffusion constant $D(T)=D_0\exp(-Q/kT)$.

In this study, we present measurements of the freezing velocity of Si(100) at large undercoolings derived from experiments on epitaxial explosive crystallization of a-Si. The present data show that the freezing velocity reaches a maximum of 15.8 m/s at large (> 130 K) undercooling. From these data the interface response functions of c-Si(100) and a-Si, $v_c(T)$ and $v_a(T)$, respectively, are investigated. The results are consistent with a DLT-formulation indicating that diffusive motion in the liquid near the interface is the rate-limiting factor in freezing of silicon. TST is not consistent with the data if the kinetic

prefactor is assumed to be limited by the sound velocity.

The experimental procedure and the results are presented in Sec. II. In Sec. III, the approach is described by which $v_c(T)$ and $v_a(T)$ are derived directly from the experimental data. Heat-flow calculations are described in Sec. IV, together with the procedures to obtain $v_c(T)$ and $v_a(T)$ for either DLT or TST from the numerical modeling. A detailed analysis of the errors arising from uncertainties in the heat-flow calculations is also presented in this section. In Sec. V the physical implications of the present analysis are discussed.

II. EXPERIMENTAL PROCEDURES

A. Experiment

Experiments were performed on Si samples consisting of a *c*-Si/*a*-Si/*c*-Si layer structure produced by ion implantation. Details on the sample preparation procedure are given in an earlier publication.[17] The 420 nm thick amorphous layer was buried beneath a 130 nm thick single-crystalline surface layer.[17] Phase transformations were induced in these samples by irradiation with a single pulse from a *Q*-switched ruby laser [wavelength 694 nm, pulse duration 32 ns full width at half maximum (FWHM)] under far-field conditions. The energy in the ≈ 1 mm diameter laser spots was laterally homogeneous to within 10%. The average energy density was determined with an accuracy of $\approx 5\%$ using calorimetry. Transient optical reflectivity[18] of the irradiated area of the sample was monitored *in situ* using a continuous-wave AlGaAs laser operating at 825 nm and focused to a $\approx 50\mu$m diameter spot.

B. Results

The transient reflectivity measured during irradiation at an energy density of 0.25 J/cm^2 shows pronounced oscillations. For a detailed description, see Refs. 17, 19, and 20. This observation is indicative of a planar solid-liquid interface moving towards the interior of the sample. The following melting and freezing scenario has been suggested.[17,19,20] During the laser pulse, the crystalline surface layer and the buried amorphous layer are rapidly heated. The optical absorption coefficient of *a*-Si is substantially higher than that of *c*-Si.[21] Moreover, the melting temperature of *a*-Si (T_{ma}) is lower than that of *c*-Si (T_{mc}), the estimated difference being 200 to 265 K.[22,23] Consequently, the laser heating initiates melting in the *a*-Si at the buried *c*-Si/*a*-Si interface, while the surface temperature remains below T_{mc}. Upon melting, the temperature of the thin liquid layer equals T_{ma}. This undercooled liquid will start to crystallize at the *c*-Si template on top. The net amorphous-to-crystalline transformation is exothermic due to the difference in latent heat of melting of *a*-Si and *c*-Si.[23] Release of this heat results in deeper melting of *a*-Si. Hence, a continuous self-sustained "explosive" crystallization (EC) process occurs,[22,24] mediated by a buried liquid layer that moves rapidly inward. As the crystalline surface layer is relatively transparent at the wavelength of the probe laser, two reflected signals are interfering; one from the sample surface and one from the buried *c*-Si/*l*-Si interface. The interference condition changes with the position of the moving liquid layer, which explains the fact that maxima and minima are observed in the reflectivity measurements. The reflectivity transient exhibits 8 extreme, indicating that the buried liquid layer propagates 350±30 nm through the *a*-Si and quenches at 480±30 nm below the surface, in agreement with TEM results.[17,19] The velocity of the freezing *c*-Si/*l*-Si interface can be obtained as a function of depth from the reflectivity oscillations.[17,19,20] The crystallization velocity appears to be constant over the total depth and the mean interface velocity has been calculated to be 15.8±0.3 m/s.[20] Cross-section TEM and channeling Rutherford backscattering spectrometry have shown that EC of the buried *a*-Si layer proceeds epitaxially.[17,19]

The laser induced processes were investigated over a wide range of energy densities.[17,19] For energy densities between 0.20 and 0.25 J/cm^2 the number of interference extrema increases with energy density, but in all cases the observed EC velocity is ≈ 16 m/s. For energy densities in excess of 0.25 J/cm^2 buried melting at the *c*-Si/*a*-Si interface is followed by melting of *c*-Si at the surface. Since the penetration depth of the probe laser in *l*-Si is only ≈ 10 nm, in that case the moving buried melt is optically shielded by the presence of the surface melt. Hence, above 0.25 J/cm^2 the EC speed could not be obtained. In additional experiments, samples consisting of different layer structures were investigated.[17] In all samples epitaxial EC is observed for appropriate energy density of the laser pulse. The measured EC speed is similar to that in the present experiment, independent of the layer structure.

III. INITIAL CONSTRAINTS

A. Procedure

In this section, a simplified interpretation of the experimental data is given in order to investigate the interface response functions $v_c(T)$ and $v_a(T)$. First, it is assumed that the activation barrier Q is the same for both the *l*-Si→*c*-Si and *l*-Si→*a*-Si transitions. Within the concept of TST this is plausible, since both transitions are between a metallic liquid and a fourfold coordinated covalently bonded solid.[25] In DLT this assumption is also reasonable, since for both cases the rate-limiting step is diffusion in the liquid. The remaining unknown parameters of the interface response functions are the common activation energy Q and the prefactors c_c and c_a of $v_c(T)$ and $v_a(T)$, respectively. In this section we bring together results of several experiments performed earlier by other investigators, as well as our data from epitaxial EC, in order to derive a set of constraints. These experimental constraints will be used in a fitting procedure from which the parameters of $v_c(T)$ and $v_a(T)$ are obtained.

Figure 1 gives a general overview of the constraints discussed in this section [points numbered (1)–(4)]. The first constraint is given by the fact that $v_a(T)$ and $v_c(T)$ are equal to zero at the equilibrium melting temperature T_{ma} and T_{mc}, respectively [(1a) and (1b) in Fig. 1]. In the present analysis, T_{ma} is taken to be 225 K below T_{mc}, in-

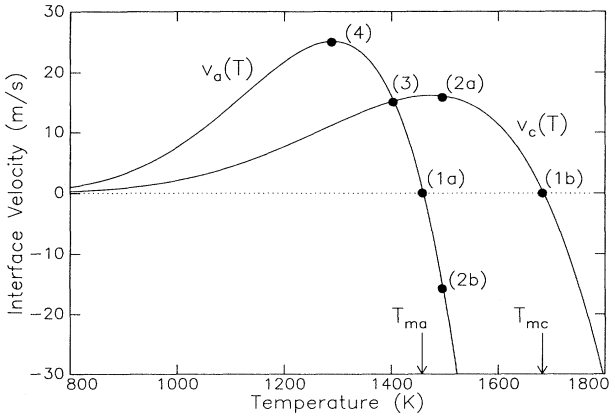

FIG. 1. Interface response functions of c-Si and a-Si derived from the experimental constraints (1)–(4) (see text). The solid points are the experimental data used in the analysis. Numbers refer to equations in the text.

termediate between the values given in Refs. 22 and 23.

The second constraint is derived from our experimental data. It is assumed that during epitaxial EC the freezing c-Si/l-Si interface and the melting l-Si/a-Si interface both are moving at the same constant velocity of 15.8 m/s. Additionally, the temperature of both interfaces is taken to be the same, which is the case if the thermal conductivity of the liquid layer separating the interfaces is infinitely high. These first-order assumptions result in the following constraint during EC:[26]

$$v_c(T_2)=15.8 \text{ m/s} , \tag{2a}$$

$$v_a(T_2)=-15.8 \text{ m/s} , \tag{2b}$$

where T_2 is the common interface temperature. Since freezing of c-Si requires undercooling the interface below T_{mc} and melting of a-Si requires overheating above T_{ma}, it is clear that $T_{ma} < T_2 < T_{mc}$.

The third constraint is obtained from the observation that freezing of l-Si on Si(100) transforms from crystallization into amorphous growth if the interface velocity exceeds 15 m/s.[27–29] In the present analysis it is assumed that this transition occurs at a certain undercooling below T_{ma} for which the amorphization velocity $v_a(T)$ increases above the crystallization velocity $v_c(T)$.[30] Hence, there must be a temperature $T_3 < T_{ma}$ at which the interface response functions $v_c(T)$ and $v_a(T)$ cross at 15 m/s:

$$v_c(T_3)=15 \text{ m/s} , \tag{3a}$$

$$v_a(T_3)=15 \text{ m/s} . \tag{3b}$$

Finally, we make use of the fact that the amorphization rate of undercooled l-Si formed by picosecond-laser irradiation is observed to saturate at a speed of approximately 25 m/s for large undercooling.[7] This implies that at a certain temperature below T_{ma} the response function of a-Si reaches a maximum of 25 m/s, leading to the following constraint:

$$v_a(T_4)=25 \text{ m/s} , \tag{4a}$$

$$\left.\frac{dv_a}{dT}\right|_{T_4}=0 , \tag{4b}$$

with $T_4 < T_{ma}$.

Equations (2)–(4) provide a set of six boundary conditions from which the six unknown parameters, i.e., the activation energy Q, the prefactors c_a and c_c, and the temperatures T_2, and T_3, and T_4, are derived.

B. Results

Figure 1 shows the curves $v_c(T)$ and $v_a(T)$ matching Eqs. (2)–(4). The curve for c-Si reaches a maximum of 15.8 m/s at (2a), at a temperature well above T_{ma}, which corresponds to Eq. (2). For lower temperatures the curve $v_c(T)$ decreases and crosses $v_a(T)$ at (3) at 15 m/s, in accordance with Eq. (3). Furthermore, the maximum in the curve of a-Si of 25 m/s is clearly reproduced [Eq. (4)]. The values obtained for the parameters Q, c_c and c_a are listed in Table I. It should be noted that the prefactors c_c and c_a are both well above the sound velocity.

In the analysis the epitaxial EC velocity [constraint (2)] was varied between 15.0 and 16.6 m/s, the amorphization velocity [constraint (3)] between 13.5 and 16.5 m/s, and the maximum speed of amorphous growth [constraint (4)] between 20 and 40 m/s. The obtained values for the activation energy Q range from 0.48 to 3.3 eV, for the prefactor c_c from 1.6×10^3 to 8.8×10^{12} m/s, and for the prefactor c_a from 5.9×10^3 to 2.4×10^{14} m/s.

TABLE I. Fit values of the activation energy Q, and the prefactors c_c and c_a in Eq. (1) obtained by different analysis procedures. λ_c and λ_a are the characteristic diffusion distances in DLT. The listed values correspond to the interface response functions $v_c(T)$ and $v_a(T)$ displayed in Fig. 1, 4, 5, and 7.

Analysis procedure	Fig.	Q (eV)	c_c (m/s)	c_a (m/s)	λ_c (Å)	λ_a (Å)
Analytical	1	0.78	1.8×10^4	8.1×10^4	$1.3\sqrt{f_c}$	$0.6\sqrt{f_a}$
Heat flow, standard	4	1.08	1.8×10^5	1.1×10^6	$1.1\sqrt{f_c}$	$0.5\sqrt{f_a}$
Heat flow, $c \le c_s$	5	0.53	3.2×10^3	8.4×10^3	$1.3\sqrt{f_c}$	$0.8\sqrt{f_a}$
Heat flow, $\kappa_l=2.1$ W/(cm K)	7	0.77	1.7×10^4	7.5×10^4	$1.3\sqrt{f_c}$	$0.6\sqrt{f_a}$
Heat flow, $\kappa_l=2.1$ W/(cm K), $c \le c_s$	7	0.50	2.2×10^3	8.4×10^3	$1.4\sqrt{f_c}$	$0.7\sqrt{f_a}$

Clearly, the uncertainties in the constraints (2) through (4) lead to a large variation in the values obtained for Q, c_c, and c_a. For certain choices even unphysically high values (e.g., in excess of the speed of light) are found for the prefactors. Nevertheless, only in a very small region in parameter space allowed by the experimental uncertainties in constraints (2) through (4) is the prefactor c_a found to be lower than the sound velocity of a-Si ($c_s \approx 8400$ m/s). As discussed in Sec. I, this is a requirement in TST. In DLT however, there is no limit to the kinetic prefactor. The analysis presented in this section therefore indicates that in most cases TST is not able to match the constraints of Eqs. (2) through (4).

In the present analysis, constraint (2) is a simplified representation of our experiments. In order to improve our test of the different kinetic models, a full elaboration of epitaxial EC was performed using numerical heat-flow calculations. This analysis is presented in the following section.

IV. NUMERICAL HEAT-FLOW CALCULATIONS

A. Procedure

From the observation of epitaxial EC more information can be extracted on the $v_c(T)$ curve near the critical point (2a) (Fig. 1). For this purpose we analyze the data of epitaxial EC discussed in Sec. II using heat-flow calculations. It will be shown that the freezing at 15.8 m/s does not occur at a fixed temperature, but in a temperature range. This has important consequences for the test of the kinetic models.

The transient phase transformations were modeled using a numerical one-dimensional finite difference method originally developed by Wood and Geist.[31] Numerical convergence was achieved for space step sizes of 5 nm. In the calculations described here, a space step size of 4 nm and time steps of 0.1 ps were used. The input parameters are the optical constants, the thermal conductivities, and the specific heats of a-Si, c-Si, and l-Si, the melting temperature and the latent heats for a-Si and c-Si, and the laser-pulse energy density. The values for the thermal and optical parameters were taken from the literature, and are discussed in detail in Ref. 21. The surface reflectivity is calculated using a Fresnel matrix formalism, which takes the multilayer structure into account.[32] In the simulations the crystallization velocity of the c-Si/l-Si interface was fixed at the experimental value of 15.8 m/s. The melting rate $v_{al}(T)$ of the l-Si/a-Si interface was assumed to vary linearly around T_{ma}: $v_{al}(T)=(T_{ma}-T)/\zeta_{al}$. The overheating parameter, ζ_{al}, is directly related to the slope of $v_a(T)$ at the melting temperature and is considered an adjustable parameter in the calculations.

The step-wise procedure used to derive $v_c(T)$ and $v_a(T)$ through the heat-flow calculations can be summarized as follows: (i) In the first step a certain value for the overheating parameter ζ_{al} is taken. (ii) This value for ζ_{al} is applied in the modeling to simulate the process of epitaxial EC. The energy density is adjusted so that the calculated quench depth of epitaxial EC is equal to what is experimentally observed (i.e., ≈ 480 nm). (iii) The modeling of epitaxial EC provides information on the temperature of the freezing interface as a function of depth during the process. The calculated temperature combined with the measured freezing velocity as a function of depth gives data points for the freezing velocity as a function of temperature. (iv) The curve $v_c(T)$ is fitted to the points obtained in step (iii) using the activation energy Q and the prefactor c_c as free parameters. (v) For the interface response function of a-Si the same activation energy Q is applied (see Sec. III A). The unknown prefactor c_a is adjusted so that the slope of $v_a(T)$ at $T=T_{ma}$ matches the value of ζ_{al} that was taken in the step (i) of the procedure.[26] (vi) Steps (i) through (v) are repeated for a large set of ζ_{al} values. In the final stage of the analysis, the value of ζ_{al} is selected for which the curve $v_a(T)$ has a maximum of ≈ 25 m/s in accordance with experiment.[7] Using this selection criterion a self-consistent set of curves $v_a(T)$ and $v_c(T)$ is obtained.

B. Results

In this section the outcome of the fitting procedure is presented step by step.

(i) In the following, the results are shown for the analysis using 2 K/(m/s) for the overheating parameter ζ_{al}. As will become clear in the final stage of the analysis, this value for ζ_{al} leads to the best fits for $v_c(T)$ and $v_a(T)$.

(ii) For the appropriate energy density of the laser pulse (0.26 J/cm^2), the simulations indicate that melting starts at the buried c-Si/a-Si interface. The melted layer solidifies from the c-Si surface seed, and it is found that the heat of crystallization that is released is indeed sufficient to melt more a-Si. Figure 2 shows the calculated position of the phase boundaries in the simulation as a function of time in a depth-phase-time diagram. Crystallization starts immediately after the generation of a thin liquid layer because the melted Si is highly undercooled with respect to T_{mc}. The freezing interface proceeds at

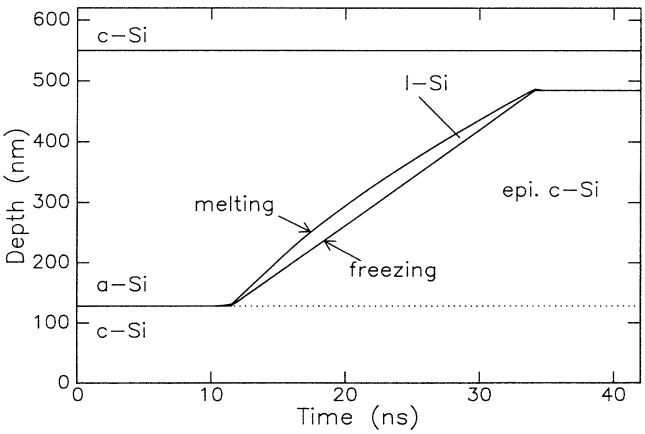

FIG. 2. Depth-phase-time diagram for epitaxial explosive crystallization obtained by heat-flow modeling using an energy density of 0.26 J/cm^2. The peak of the laser pulse (32 ns FWHM) is taken as the origin of the time axis.

15.8 m/s. The latent heat released at the freezing interface drives the melting interface inwards at a calculated initial speed of ≈ -21 m/s. As the liquid layer approaches the c-Si substrate during EC, an increasing amount of the released heat is lost to the substrate through the heat conduction. As a consequence the melting rate decreases with increasing depth, until the liquid layer finally vanishes at a total depth of ≈ 485 nm. This calculated quench depth is in agreement with experiment, indicating that for the energy density used, the heat-flow calculations give a satisfactory modeling of epitaxial EC. In fact, this energy density is in exact agreement with the experimental value as determined by calorimetry (Sec. II).

(iii) As a result, the heat-flow calculations give quantitative information on the temperature distribution throughout the process. The temperature of both the freezing interface and the melting interface are shown in Fig. 3. When buried melting takes place, the temperature of the liquid is close to T_{ma}. However, the interface temperature is instantaneously increased as crystallization starts, due to the release of latent heat. The temperature of the melting interface jumps ≈ 42 K above T_{ma}, the amount of overheating corresponding to an initial melting rate of ≈ -21 m/s [note that $\zeta_{al}=2$ K/(m/s)]. As the melting rate decreases with depth, the interface temperature decreases to lower overheating above T_{ma}. Figure 3 also shows that the temperature of the freezing interface is significantly higher than the temperature of the melting interface throughout the entire process of epitaxial EC. This is because the large release of latent heat at the freezing interface, combined with the finite thermal conductivity of l-Si, induces a considerable temperature gradient in the liquid layer. Small temperature variations are superimposed on the gradual temperature excursion of both freezing and melting interface. This is a direct consequence of the fact that the calculated surface reflectivity oscillates due to the motion of the buried melt, which induces oscillations in the energy input from the tail of the laser pulse. The maximum temperature of the freezing interface of $T \approx 1545$ K, corresponding to ≈ 140 K undercooling below T_{mc}, is reached at a depth of 250 nm. Beyond this maximum the interface temperature decreases with depth until finally epitaxial EC is quenched. By combining the experimentally obtained freezing velocity for each depth (Sec. II) with the calculated interface temperature (Fig. 3), the relation between freezing velocity and temperature can be established for $\zeta_{al}=2$ K/(m/s). These data are shown in Fig. 4. The result shows that the freezing velocity does not depend on the degree of undercooling over a temperature plateau, ranging from ≈ 1500 to ≈ 1550 K.

(iv) The interface response curve $v_c(T)$ was fitted through the data set using the prefactor c_c and activation energy Q as free parameters, and the result is shown in Fig. 4 with $Q=1.08$ eV and $c_c=1.8\times 10^5$ m/s. The inset in Fig. 4 shows the data points with their error bars together with the fitted curve. It is clear that the observed plateau in the freezing data is well reproduced by the calculated $v_c(T)$ curve.

(v) The slope of $v_a(T)$ at the melting temperature was matched with $\zeta_{al}=2$ K/(m/s), using the value for the activation energy Q obtained under (iv). The required value for the prefactor c_a is 1.1×10^6 m/s.

(vi) The calculated $v_a(T)$ curve in Fig. 4 displays a maximum amorphization velocity of ≈ 27 m/s, which is close to the experimentally observed maximum.[7] Moreover, the curves for $v_c(T)$ and $v_a(T)$ cross at ≈ 14 m/s, which is in agreement with the experimental observation that undercooled l-Si solidifies into a-Si above 15 ± 1.5 m/s [constraint (3)].[27] This indicates that $\zeta_{al}=2$ K/(m/s) leads to a set of curves $v_c(T)$ and $v_a(T)$, which gives a consistent description of the present data as well as earlier experiments. ζ_{al} values different from 2.0 ± 0.5 K/(m/s) do not lead to satisfactory agreement with experiment.

The values for the best fit parameters are listed in Table I. The obtained prefactors for $v_c(T)$ and $v_a(T)$ are considerably higher than the sound velocity (8433 and

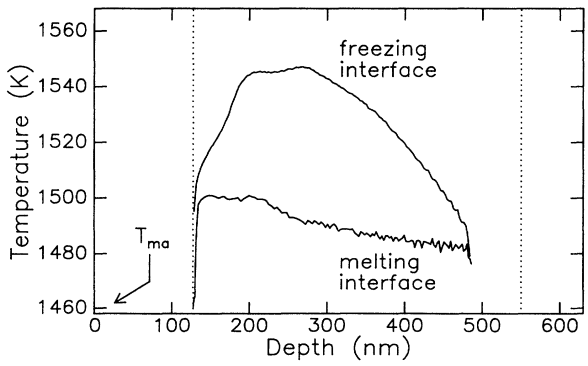

FIG. 3. Calculated temperature of the freezing c-Si/l-Si interface and the melting l-Si/a-Si interface as a function of the interface depth obtained by the standard heat-flow modeling [$\zeta_{al}=2$ K/(m/s)].

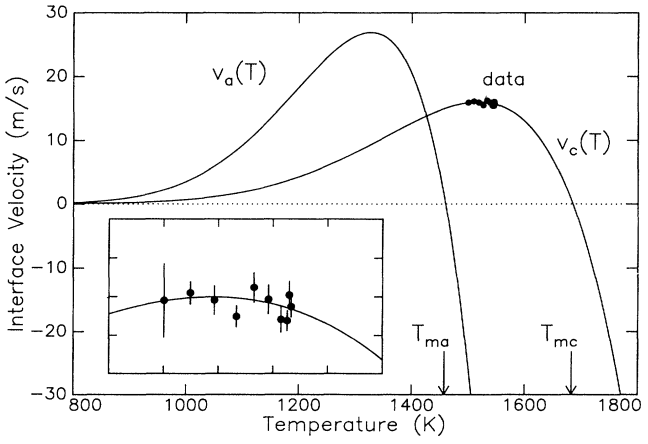

FIG. 4. Interface velocity as a function of temperature. Circles are the data derived from the experimental velocity data and the calculations in Fig. 3. The drawn lines are the fitting curves for the response functions of c-Si and a-Si. The inset shows an enlarged view of the data and the fit.

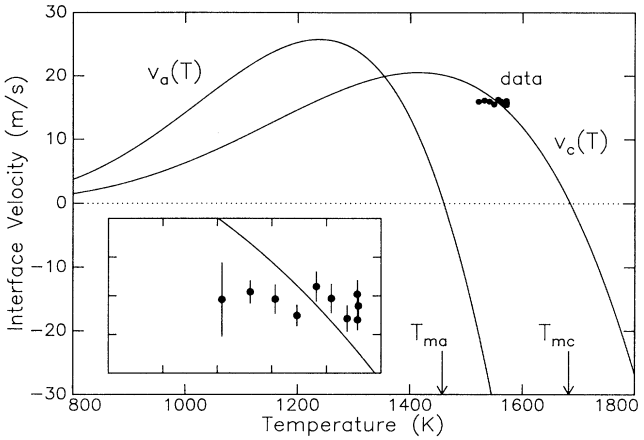

FIG. 5. Data and fitting curves for the interface velocity as a function of temperature. Circles are the data calculated for $\zeta_{al}=3$ K/(m/s). In the analysis the prefactors of the response functions were limited by the sound velocity. The inset shows an enlarged view of the data and the fit.

8400 m/s for *c*-Si and *a*-Si, respectively). This indicates that TST does not give a self-consistent description of the data. Instead, the high values for c_c and c_a can be interpreted in terms of the DLT model, and the results for the characteristic diffusion distance λ are given in Table I. This will be discussed in detail in Sec. V.

As a further test of TST, an additional fitting sequence was performed in which the allowed values for c_c and c_a were restricted by the sound velocity. In that case the best value for the overheating parameter ζ_{al} is 3 K/(m/s), which results in a plateau in the freezing velocity ranging from $\approx$1520 to $\approx$1570 K. Figure 5 shows the data and the fitting curves obtained for $v_c(T)$ and $v_a(T)$. The fitting parameters are listed in Table I. The inset in Fig. 5 clearly shows that $v_c(T)$ does *not* fit the freezing data. In addition, $v_c(T)$ and $v_a(T)$ cross at $\approx$20 m/s, which is inconsistent with the experimental constraint of Eq. (3). It should be noted that also the entropy-limited formulation of TST is inconsistent with the data since in this theory, the limit to the prefactor is even further reduced below c_s by the entropy term.

C. Error analysis

1. Parameter inaccuracy

Not all thermodynamical and optical parameters employed in the simulations are known very accurately. Changing the parameters influences the calculated temperature profiles (as in Fig. 3), which then could change the outcome of the fitting procedure. The results obtained for variation of the thermal conductivity of *l*-Si (κ_l) and *a*-Si (κ_a) are presented in detail in the following paragraphs. All other parameters were independently varied within their uncertainty range and simulations were performed with a fixed value of the overheating parameter [i.e., $\zeta_{al}=2$ K/(m/s)]. The energy density was taken such that the calculated quench depth would reproduce the experimental value of $\approx$480 nm. In all cases the calculated temperature excursion does not deviate more than 10 K from the profile shown in Fig. 3. This implies that the outcome of the fitting procedure is not significantly affected by the inaccuracy of these parameters.

2. Thermal conductivity of l-Si

The heat flow in the liquid layer between the freezing and the melting interface is determined by the thermal conductivity of the liquid, κ_l. In the "standard" simulation (Figs. 2 and 3), a temperature dependent κ_l is used, calculated from the electrical conductivity using the Wiedemann-Franz law.[21] This gives $\kappa_l=0.47$ W/(cm K) at $T=T_{mc}$. Measured values for κ_l range from 0.69 to 2.1 W/(cm K).[33,34] It is likely that the latter κ_l value is too high, since the value for the thermal conductivity of *c*-Si reported in Ref. 33 is too high as well, as discussed in detail in Ref. 34. Nevertheless, for completeness simulations have been performed employing $\kappa_l=2.1$ W/(cm K). This is shown in Fig. 6, which displays the temperature of the melting and the freezing interface calculated with $\zeta_{al}=2.5$ K/(m/s) and an energy density of 0.26 J/cm^2. These choices for ζ_{al} and the energy density again are optimum values found using the procedure of Sec. IV A. It is clear that the temperature excursion of the melting interface is similar to that obtained in the standard calculation (Fig. 3). In addition, Fig. 6 shows that the temperature difference between the freezing and the melting interface is drastically reduced, which is a consequence of the increased heat conduction in the liquid. The calculated temperature of the *freezing* interface however still varies between 1490 and 1520 K. This is related to the fact that the *melting* interface exhibits a temperature excursion due to the nonzero value of ζ_{al}.

The data for $v_c(T)$, obtained by combining the calculated temperature excursion (Fig. 6) with the velocity data (Sec. II), are shown in Fig. 7. The temperature range for which the freezing velocity is constant has a width of $\approx$30 K. In addition to the data, Fig. 7 shows the best fits for $v_c(T)$ and $v_a(T)$, which agree well with

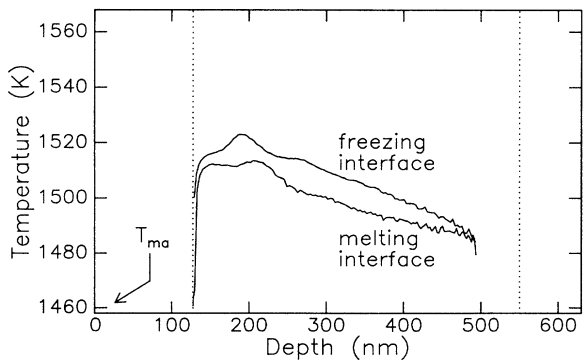

FIG. 6. Calculated temperature of the freezing *c*-Si/*l*-Si interface and the melting *l*-Si/*a*-Si interface as a function of the interface depth using 2.1 W/(cm K) for the thermal conductivity of *l*-Si.

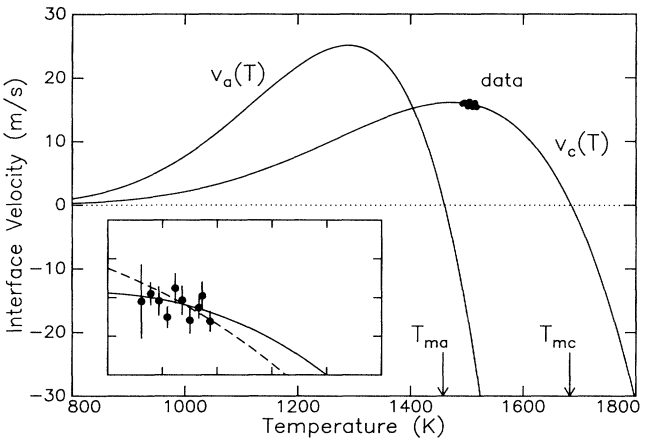

FIG. 7. Data and fitting curves for the interface velocity as a function of temperature. Circles are the data calculated using 2.1 W/(cm K) for the thermal conductivity of *l*-Si (Fig. 6). The inset shows an enlarged view of the data. The dashed line shows the best fit for the response function of *c*-Si for which the prefactor was limited by the sound velocity.

the calculated data and the experimental crossing point of Eq. (3). The fitting parameters are listed in Table I.

The dashed line in the inset of Fig. 7 shows the $v_c(T)$ curve obtained from the analysis in which the prefactors of both $v_c(T)$ and $v_a(T)$ are limited by the sound velocity to test TST. The fitting parameters are also listed in Table I. In this case also, the $v_c(T)$ curve fits the data obtained for the high κ_1 value. This indicates that in this case TST is applicable, but it is again pointed out that the κ_1 value used is unrealistically high. In addition, using TST and the high κ_1 value in the analysis, the obtained curves for $v_c(T)$ and $v_a(T)$ do not reproduce the constraint of Eq. (3), as they cross at ≈ 18 m/s (not shown).

3. *Thermal conductivity of a-Si*

The heat released at the freezing interface during epitaxial EC is partly used to melt the *a*-Si in front of the liquid. In addition, heat is lost to the crystalline substrate by thermal diffusion. The heat flux at any depth in the *a*-Si layer is given by the product of the thermal conductivity of *a*-Si, κ_a, and the local temperature gradient. As the liquid layer approaches the well-conducting *c*-Si substrate, the temperature gradient in the *a*-Si layer must become steeper. The heat flow from the liquid to the substrate increases, and the amount of energy available for melting is reduced. Hence, the melting rate slows down, which finally leads to quenching of the process. This effect is clearly illustrated in the simulation shown in Fig. 2, which was obtained using $\kappa_a = 0.01$ W/(cm K). Experimental values for κ_a range from 0.005 to 0.026 W/(cm K).[35–39] It should be noted that these values are often averages over a certain temperature and values close to T_{ma} are not known. An extreme suggestion is that near T_{ma}, κ_a approaches the value for *c*-Si.[40]

In the present simulations κ_a was varied between 0.005 and 0.1 W/(cm K). The calculated quench depth is shown as a function of κ_a in Fig. 8 for energy densities of 0.22, 0.25, 0.30, and 0.50 J/cm^2. For the lowest κ_a value [0.005 W/(cm K)] the quench depth is ≈ 500 nm for all energy densities, which indicates that almost the complete *a*-Si layer has crystallized. Figure 8 shows that the quench depth decreases considerably with increasing κ_a. This is due to the fact that for increasing κ_a the amount of heat available for melting of *a*-Si is reduced, because during EC a higher heat fraction is conducted from the liquid to the substrate. In simulations using densities of 0.22 J/cm^2 with $\kappa_a \geq 0.013$ W/(cm K), 0.25 J/cm^2 with $\kappa_a \geq 0.03$ W/(cm K), and 0.30 J/cm^2 with $\kappa_a \geq 0.05$ W/(cm K) no epitaxial EC is observed to occur. In these cases the heat conduction is so high that the supplied energy is not sufficient to initiate buried melting in the sample.

Now we will compare the data in Fig. 8 to the experimentally observed quench depth of 280±30 nm for an energy density of ≈ 0.22 J/cm^2, and 480±30 nm for ≈ 0.25 J/cm^2 (solid points in Fig. 8).[17] As is clear from Fig. 8, the experimental quench depths are reproduced by the simulations if $\kappa_a \approx 0.01$ W/(cm K) is used. Taking the experimental uncertainty in the energy density into account, the appropriate value for κ_a is found to range from 0.005 to 0.02 W/(cm K). Indeed, this estimate for κ_a is in agreement with estimates based on a wide variety of other experiments.[35–39] Moreover, for all simulations shown in Fig. 8 which yield a quench depth of ≈ 480 nm, the temperature excursions are similar to the curve plotted in Fig. 3 within 10 K, regardless of the values used for κ_a and the energy density. Additional simulations were performed to investigate the possible influence of a strongly temperature dependent κ_a. As a functional form, we

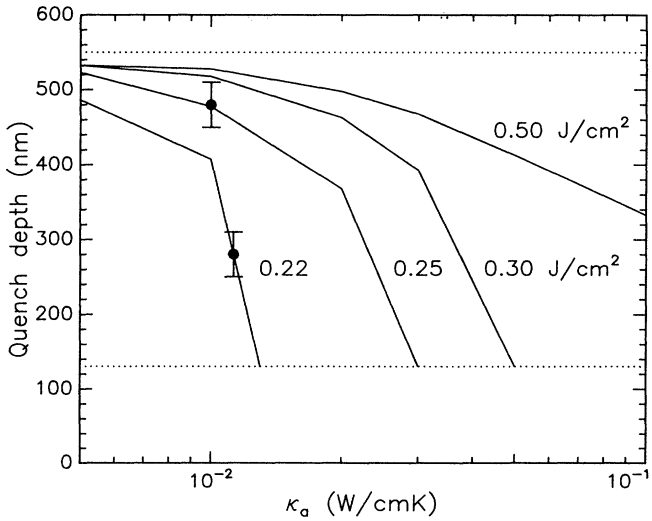

FIG. 8. Calculated quench depth as a function of the thermal conductivity of *a*-Si. The solid lines represent calculations using energy densities of 0.22, 0.25, 0.30, and 0.50 J/cm^2 (indicated in the graph). The solid prints represent experimentally observed quench depths for 0.22 and 0.25 J/cm^2.

have chosen

$$\kappa_a(T)=0.005\times \exp(4T^2/T_{ma}^2)\ \mathrm{W/(cm\,K)}\ ,$$

for which κ_a approaches the thermal conductivity of c-Si at $T=T_{ma}$. The quench depth is calculated to be 465 nm for an energy density of 0.36 J/cm^2. Again, the calculated temperature excursion of the freezing interface does not deviate considerably from Fig. 3.

These results indicate that if the simulations are forced to match experiment in terms of the quench depth, the calculated interface temperature does not depend strongly on κ_a. Therefore, our conclusions are not affected significantly by the used value of the thermal conductivity of a-Si.

V. DISCUSSION

The present study of epitaxial EC shows that liquid silicon crystallizes on Si(100) at a velocity of 15.8 m/s for a range of temperatures between T_{ma} and T_{mc}. The precise range can be derived from heat-flow modeling. Fitting the interface response functions $v_c(T)$ and $v_a(T)$ to these semiempirical velocity-temperature data requires values for the prefactors larger than the sound velocity c_s, unless an unrealistically high value for the thermal conductivity of l-Si is used in the simulations. The data are consistent with the DLT model in which there is no fundamental limit to the kinetic prefactor. It should be noted that the data are also consistent with a recently developed theory[41] in which the density difference between liquid and solid Si is assumed to influence the freezing velocity.[20] In this model also, diffusion in the liquid is the rate-limiting factor for freezing.

The results indicate that the activation energy involved in the phase transformation is $Q=0.7-1.1$ eV. In the DLT, Q equals the activation energy for self-diffusion of atoms in the liquid near the liquid-solid interface. The obtained value for Q is high when compared to the activation energy for self-diffusion in elemental metallic liquids.[42] This suggests that the liquid near the interface does not exhibit pure metallic behavior. Indeed, molecular-dynamic studies[43] have suggested that l-Si has a lower average coordination number than most liquid metals, due to the persistence of some covalent bonding in the liquid. Additionally, the solid on one side of the interface might cause some local ordering in the liquid,[44] increasing the barrier for self-diffusion. Note that the activation energy for self-diffusion in c-Si is 4 eV.[45]

The other essential parameter in the DLT is the characteristic diffusion distance λ, which is related to the prefactor c through $\lambda=\sqrt{D_0 d/c}\,\sqrt{f}$. An estimate for D_0 is obtained by assuming that the diffusion near the interface can be described by the bulk liquid diffusion constant.[46] The fitting results of the analytical approach (Fig. 1) are $\lambda_c=1.3\sqrt{f_c}$ Å for crystalline growth and $\lambda_a=0.6\sqrt{f_a}$ Å for amorphous growth (see Table I). The analysis based on the heat-flow modeling (Fig. 4) gives $\lambda_c=1.1\sqrt{f_c}$ Å and $\lambda_a=0.5\sqrt{f_a}$ Å. The active site fraction for the Si(100)/l-Si interface (f_c) and the a-Si/l-Si interface (f_a) are unknown, which obstructs a direct comparison of the values of λ obtained for $v_c(T)$ and $v_a(T)$. However, for both the crystalline and the amorphous growth the diffusion distance is smaller than the atomic distance in the solid. This indicates that only a small local rearrangement of atoms in the liquid near the interface is required for attachment to the solid.

A test of TST based on transient conductance (TC) measurements led to the conclusion that a good description of $v_c(T)$ and $v_a(T)$ was obtained for the entropy-limited formulation of TST, employing an activation energy lower than 0.25 eV.[4] However, this theory is not able to consistently reproduce our experimentally determined freezing data at 15.8 m/s. This needs further investigation.

The DLT curve of c-Si can be compared with the analysis of TC measurements in the temperature range near T_{mc}.[2,3] From these measurements the undercooling parameter ζ_{lc} of $v_c(T)$ is estimated to be 15 ± 5 K/(m/s) (Ref. 2) and 17 ± 3 K/(m/s) (Ref. 3), considerably different from that of the DLT curve in this paper [$\zeta_{lc}\approx4$ K/(m/s)]. On the other hand, picosecond-laser measurements presented in the same work yield $\zeta_{lc}\approx4$ K/(m/s),[3] whereas the analysis of x-ray measurements give $\zeta_{lc}=3.3\pm1.7$ K/(m/s),[6] both in good agreement with our analysis. Apparently, a large discrepancy exists in the results from different experimental techniques. The origin of this controversy is still unclear and might be an interesting subject of future experiments.[6]

Finally, the present findings are confirmed by results from molecular-dynamics modeling of freezing in silicon,[12] in which the calculated freezing velocity was found to reach a maximum of ≈18 m/s at large undercooling, and the activation energy for the self-diffusion of atoms in l-Si was determined to be rather high ($Q=0.56$ eV). In that study the calculated freezing data were perfectly reproduced by DLT.

VI. CONCLUSIONS

Experimental data obtained from epitaxial explosive crystallization of amorphous silicon have been used to test different theories describing the kinetics of freezing in silicon. The freezing velocity of Si(100) saturates at 15.8 ± 0.3 m/s for large undercooling (>130 K) below the c-Si melting temperature. The best agreement between theory and experiment is obtained if the freezing rate at the solid is assumed to be limited by the diffusive motion of atoms in the liquid in the vicinity of the interface. The activation energy for self-diffusion of atoms in the liquid near the interface is estimated to be 0.7–1.1 eV. This suggests nonmetallic behavior or some local ordering in the liquid near the interface. The average distance that atoms have to diffuse in order to attach to the solid is less than the interatomic distance in the solid. Transition state theory is not able to reproduce the experimental data if the maximum interface velocity is taken to be limited by the sound velocity.

ACKNOWLEDGMENTS

We gratefully thank R. F. Wood and G. A. Geist (ORNL, Oak Ridge) for making the heat-flow code available, D. Stock (University of Jena, Germany) for contrib-

uting to the heat-flow calculations, J. S. Custer, D. Frenkel, and F. W. Saris (FOM), and J. Y. Tsao (Sandia, Albuquerque) for fruitful discussions. This work is part of the research program of the Stichting voor Fundamenteel Onderzoek der Materie (FOM) and was made possible by financial support from the Nederlandse Organisatie voor Wetenschappelijk Onderzoek (NWO) and the Stichting der Technische Wetenschappen (STW).

*Present address: Netherlands Energy Research Foundation, Petten, The Netherlands.

[1]F. Spaepen and D. Turnbull, in *Laser Annealing of Semiconductors,* edited by J. M. Poate and J. W. Mayer (Academic, New York, 1982).

[2]G. J. Galvin, J. W. Mayer, and P. S. Peercy, Appl. Phys. Lett. **46**, 644 (1985).

[3]M. O. Thompson, P. H. Bucksbaum, and J. Bokor, in *Energy Beam-Solid Interactions and Transient Thermal Processing,* edited by D. K. Biegelsen, G. A. Rozganyi, and C. V. Shank, MRS Symposia Proceedings No. 35 (Materials Research Society, Pittsburgh, 1985), p. 181.

[4]J. Y. Tsao, M. J. Aziz, M. O. Thompson, and P. S. Peercy, Phys. Rev. Lett. **56**, 2712 (1986).

[5]J. Y. Tsao, P. S. Peercy, and M. O. Thompson, J. Mater. Res. **2**, 91 (1987).

[6]B. C. Larson, J. Z. Tischler, and D. M. Mills, J. Mater. Res. **1**, 144 (1986).

[7]P. H. Bucksbaum and J. Bokor, Phys. Rev. Lett. **53**, 182 (1984).

[8]F. F. Abraham and J. Q. Broughton, Phys. Rev. Lett. **56**, 734 (1986).

[9]U. Landman, W. D. Luedtke, M. W. Ribarsky, R. N. Barnett, and C. L. Cleveland, Phys. Rev. B **37**, 4637 (1988).

[10]W. D. Luedtke, U. Landman, M. W. Ribarsky, R. N. Barnett, and C. L. Cleveland, Phys. Rev. B **37**, 4647 (1988).

[11]M. D. Kluge and J. R. Ray, Phys. Rev. B **39**, 1738 (1989).

[12]M. H. Grabow, G. H. Gilmer, and A. F. Bakker, in *Atomic Scale Calculations in Materials Science,* edited by J. Tersoff, D. Vanderbilt, and V. Vitek, MRS Symposia Proceedings No. 141 (Materials Research Society, Pittsburgh, 1989), p. 349.

[13]A measured value for the sound velocity of *a*-Si is 6370 m/s [from I. R. Cox-Smith, H. C. Liang, and R. O. Dillon, J. Vac. Sci. Technol. A **3**, 674 (1985)], which was measured on deposited *a*-Si, which can be of quite different structure than ion-implanted *a*-Si.

[14]J. S. Custer (private communication). The sound velocity is calculated using $c_s=\sqrt{(C_{11}/\rho_a)}$, with the elastic modulus C_{11} obtained self-consistently using the Youngs modulus from S. I. Tan, B. S. Berry, and B. L. Crowder, Appl. Phys. Lett. **20**, 88 (1972), and the Rayleigh wave velocity from R. Vacher, H. Sussner, and M. Schmidt, Solid State Commun. **34**, 279 (1980). The mass density of *a*-Si, ρ_a, is taken from J. S. Custer, M. O. Thompson, D. C. Jacobson, J. M. Poate, S. Roorda, W. C. Sinke, and F. Spaepen, Appl. Phys. Lett. (to be published).

[15]H. A. Wilson, Proc. Cambridge Philos. Soc. **10**, 25 (1898).

[16]J. Frenkel, Phys. Z. Sowjetunion **1**, 498 (1932).

[17]A. Polman, P. A. Stolk, D. J. W. Mous, W. C. Sinke, C. W. T. Bulle-Lieuwma, and D. E. W. Vandenhoudt, J. Appl. Phys. **67**, 4024 (1990).

[18]D. H. Auston, C. M. Surko, T. N. C. Venkatesan, R. E. Slusher, and J. A. Golovchenko, Appl. Phys. Lett. **33**, 437 (1978).

[19]P. A. Stolk, A. Polman, W. C. Sinke, C. W. T. Bulle-Lieuwma, and D. E. W. Vandenhoudt, in *Ion Beam Processing of Advanced Electronic Materials,* edited by N. W. Cheung, A. D. Marwick, and J. B. Roberto, MRS Symposia Proceedings No. 147 (Materials Research Society, Pittsburgh, 1990), p. 179.

[20]P. A. Stolk, A. Polman, and W. C. Sinke, in *Beam-Solid Interactions: Physical Phenomena,* edited by J. A. Knapp, P. Borgesen, and R. A. Zuhr, MRS Symposia Proceedings No. 157 (Materials Research Society, Pittsburgh, 1990), p. 363.

[21]R. F. Wood and G. E. Jellison, in *Semiconductors and Semimetals,* edited by R. F. Wood, C. W. White, and R. T. Young (Academic, New York, 1984), Vol. 23 pp. 188–194.

[22]M. O. Thompson, G. J. Galvin, J. W. Mayer, P. S. Peercy, J. M. Poate, D. C. Jacobson, A. G. Cullis, and N. G. Chew, Phys. Rev. Lett. **52**, 2360 (1984).

[23]E. P. Donovan, F. Spaepen, D. Turnbull, J. M. Poate, and D. C. Jacobson, Appl. Phys. Lett. **42**, 698 (1983).

[24]W. C. Sinke and F. W. Saris, Phys. Rev. Lett. **53**, 2121 (1984).

[25]D. Turnbull, J. Phys. (Paris) Colloq. **43**, C1-259 (1982).

[26]It is implicitly assumed that there is no asymmetry in the freezing and melting velocity for small deviations from T_{ma}, so that the slope of the interface response function is continuous through $T=T_{ma}$.

[27]M. O. Thompson, J. W. Mayer, A. G. Cullis, H. C. Webber, N. G. Chew, J. M. Poate, and D. C. Jacobson, Phys. Rev. Lett. **50**, 896 (1983).

[28]A. G. Cullis, N. G. Chew, H. C. Webber, and D. J. Smith, J. Cryst. Growth **68**, 624 (1984).

[29]J. A. Yater and M. O. Thompson, Phys. Rev. Lett. **63**, 2088 (1989).

[30]J. A. Yater and M. O. Thompson, in *Kinetics of Phase Transformations,* edited by M. O. Thompson, M. J. Aziz, and G. B. Stephenson, MRS Symposia Proceedings No. 205 (Materials Research Society, Pittsburgh, 1992), p. 93.

[31]R. F. Wood and G. A. Geist, Phys. Rev. B **34**, 2606 (1986).

[32]M. Born and E. Wolf, *Principles of Optics,* 6th ed. (Pergamon, London, 1975), Chap. 1.

[33]M. G. Mil'vidskii and V. V. Eremeev, Fiz. Tverd. Tela (Leningrad) **6**, 2457 (1964) [Sov. Phys. Solid State **6**, 1949 (1964)].

[34]Y. M. Shaskov and V. P. Grishin, Fiz. Tverd. Tela (Leningrad) **8**, 567 (1966) [Sov. Phys. Solid State **8**, 447 (1966)].

[35]H. J. Goldsmid, M. M. Kaila, and G. L. Paul, Phys. Status Solidi A **76**, K31 (1983).

[36]D. H. Lowndes, R. F. Wood, and J. Narayan, Phys. Rev. Lett. **52**, 561 (1984).

[37]S. de Unamuno and E. Fogarassy, Appl. Surf. Sci. **36**, 1 (1989).

[38]M. G. Grimaldi, P. Baeri, and M. A. Malvezzi, Phys. Rev. B **44**, 1546 (1991).

[39]W. Wesch, T. Bachmann, and F. Hagemann, Nucl. Instrum. Methods B **53**, 173 (1991).

[40]M. O. Thompson (private communication).

[41]P. M. Richards, Phys. Rev. B **38**, 2727 (1988).

[42]M. Shijomi, *Liquid Metals* (Academic, New York, 1977), p. 193.

[43]I. Stich, R. Car, and M. Parrinello, Phys. Rev. Lett. **63**, 2240 (1989).

[44]U. Landman, R. N. Barnett, C. L. Cleveland, and R. H. Rast, J. Vac. Sci. Technol. A **3**, 1574 (1985).

[45]J. Hirvonen and A. Antilla, Appl. Phys. Lett. **35**, 703 (1979).

[46]For a given value of Q, the prefactor for diffusion, D_0, is calculated from the published diffusion coefficient of *l*-Si at $T=T_{mc}$:

$$D(T_{mc})=D_0\times\exp(-Q/kT_{mc})=1\times10^{-4}\ \text{cm}^2/\text{s}\ \text{(Ref. 1)}.$$

The spacing between (100) planes d is 1.36 Å.